Scripta Materialia 108 (2015) 19–22

Contents lists available at ScienceDirect

Scripta Materialia

journal homepage: www.elsevier.com/locate/scriptamat

Monte Carlo and molecular dynamics simulations of screw dislocation locking by Cottrell atmospheres in low carbon Fe–C alloys

R.G.A. Veiga [a,*], H. Goldenstein [a], M. Perez [b], C.S. Becquart [c]

[a] Escola Politécnica/Departamento de Engenharia Metalúrgica e de Materiais, Universidade de São Paulo, Av. Prof. Mello de Morais, 2463, Butantã CEP 05508-030, São Paulo/SP, Brazil
[b] Université de Lyon, INSA-Lyon, MATEIS, UMR CNRS 5510, 25 avenue Jean Capelle, F69621 Villeurbanne, France
[c] Unité Matériaux et Transformations (UMET), Ecole Nationale Supèrieure de Chimie de Lille, UMR CNRS 8207, Bat. C6, F59655 Villeneuve d'Ascq Cedex, France

ARTICLE INFO

Article history:
Received 13 April 2015
Revised 30 May 2015
Accepted 9 June 2015
Available online 10 June 2015

Keywords:
Cottrell atmosphere
Screw dislocation
Strain ageing
Monte Carlo
Molecular dynamics

ABSTRACT

On-lattice Monte Carlo shows strong carbon segregation at a screw dislocation in bcc iron for carbon contents that vary from 20 to 500 ppm, typical in ultra low and low carbon steels. Molecular dynamics simulations are then carried out using the atomic coordinates of equilibrated Cottrell atmospheres. The stresses required to make the screw dislocation break free of the carbon cloud are very high compared to carbon in solid solution; the locking time is also much longer. All simulations are performed at 300 K.

Static strain ageing (SSA) refers to the hardening of a material that has undergone plastic deformation and is then aged for a certain period of time. The underlying atomistic mechanism behind SSA, according to the theory proposed by Cottrell and Bilby [1], is the segregation of solute atoms to dislocations forming the so-called "Cottrell atmospheres", which hinders dislocation motion. Higher stresses are then required to free the dislocations. SSA is of great importance for a number of applications of metallic alloys. It is, for instance, the phenomenon behind the bake-hardenable [2–4] and quenched-and-partitioned [5] steels used in the automotive industry. Despite being an old topic in physical metallurgy, the study of the role of solute-dislocation interactions in steel plasticity has benefited from advances in experimental characterization and computational methods, as can be seen in recent works [4,6,7].

Cottrell and Bilby treated carbon atoms as hydrostatic dilatation centers and used Maxwell–Boltzmann statistics to predict both the atmosphere formation and the associated hardening. This model fails to handle site saturation (i.e., for high carbon contents, it predicts many carbon atoms at the same octahedral site). To overcome this limitation, other authors rather used Fermi–Dirac statistics [8–11]. However, since Fermi–Dirac statistics assumes non-interacting particles, it also results in unrealistically high carbon concentrations in the dislocation core, where carbon–carbon interactions play an important role. More recently, Veiga et al. [12] combined Louat formulation with an estimate of the saturation concentration in the dislocation core to improve the description of carbon occupancies near dislocations. All these models are very crude approximations and none of them considered properly the wide range of elastic/chemical interactions within the atmosphere.

Carbon interaction with the tensile stress field of edge dislocations is stronger than with the pure shear stress field of screw dislocations [12,13]. Molecular dynamics simulations were used to model the effect of a single carbon atom [14] and many carbon atoms in solid solution [7] on the glide of an edge dislocation. Given the prominent role of screw dislocations in the plasticity of iron, it is also worth studying the effect of carbon in their mobility. The binding energy of a single carbon atom to a screw dislocation reaches 0.41 eV [13,15], thus it may behave as an important carbon sink. In this work, Monte Carlo (MC) is employed to build Cottrell atmospheres around a $\frac{1}{2}[1\,1\,1](1\,1\,\bar{2})$ screw dislocation in bcc iron. Based on an appropriate interatomic potential, this approach circumvents most of the weaknesses of the simplest models mentioned above. The dislocation unpinning from the resulting carbon cloud, in turn, is simulated by molecular dynamics (MD). We used in all simulations a simulation box built according to the following procedure. The carbon-free simulation box consists of about 250,000 iron atoms arranged on a bcc lattice with

* Corresponding author.
E-mail address: rgaveiga@usp.br (R.G.A. Veiga).

http://dx.doi.org/10.1016/j.scriptamat.2015.06.012
1359-6462/

lattice parameter $a_0 = 0.286$ nm. The approximate simulation box volume is $15 \times 20 \times 10\,\text{nm}^3$, with the axis oriented in the $(1\,1\,\bar{2})$, $(1\,\bar{1}\,0)$ and $(1\,1\,1)$ directions. A screw dislocation was inserted in the center of the simulation box with the dislocation line parallel to the $(1\,1\,1)$ direction. The screw dislocation was created using the anisotropic elasticity theory as implemented in the Babel code [16]. Periodic boundary conditions are used along the $(1\,1\,1)$ and $(1\,1\,\bar{2})$ directions, following the procedure proposed by Osetsky and Bacon [17]. Free surfaces are used in the $(1\,\bar{1}\,0)$ direction.

Atomic interactions are described by an embedded atom method (EAM) [18] Fe–C potential. The Fe–Fe part [19] reproduces fairly well the core of a screw dislocation in bcc iron compared to first principles calculations. To take into account the Fe–C and C–C interactions, we used the interatomic potential initially proposed by Becquart and Raulot [20] and later modified by Veiga et al. [21]. Despite the lack of C–C pairwise interaction explicitly implemented in the interatomic potential, the manybody part of it has shown to be able to account for the C–C interactions in the iron matrix in good agreement with *ab initio* calculations [21,22]. This Fe–C potential has been widely used to model Fe–C systems, with a particular focus on carbon-dislocation interactions [20,15,13,23–25,12,7].

On-lattice MC in the NVT ensemble is used to model the equilibrium Cottrell atmosphere as a function of the carbon content c_0. Carbon atoms occupy octahedral sites in the bcc iron matrix, with the maximum occupancy of one carbon atom per site. The MC algorithm maps all the N octahedral sites found in the simulation box defined above into the components of a vector $\mathbf{q} = \{q_1, q_2, q_3, \ldots, q_N\}$. In the first MC iteration, given the amount of carbon atoms initially in solid solution, the values of a number of randomly chosen components of $\mathbf{q}$ are set to 1 (occupied) and the remaining are set to 0 (empty). At every subsequent MC iteration, the code selects a component $q_i = 1$ and changes its value to 0; then a component $q_j = 0$ has 1 assigned to it. Hence the allowed MC move consists of exchanging the occupations of two octahedral sites. Both i and j are positive integer indexes chosen at random; however, in order to enhance the sampling in the vicinity of the dislocation, the selection of the empty site is biased by assigning different probabilities $\{w_j\}$ to the components $\{q_j\} = 0$, as shown below:

$$w_j = \frac{\mathrm{e}^{-\mu r_j}}{W} \tag{1}$$

In Eq. (1), μ is a parameter that defines the steepness of the bias, r_j is the distance of the jth octahedral site from the dislocation line and $W = \sum_{k=1}^{N} \mathrm{e}^{-\mu r_k}$ normalizes the probability. In this work, we used $\mu = 0.005\ \text{nm}^{-1}$; this value implies that the probability of choosing an empty site within 5 nm from the dislocation line is about 50%. After the MC move, $\mathbf{q}$ is remapped into the fresh simulation box, with carbon atoms being inserted at the octahedral sites that correspond to the components $\{q_i\} = 1$. The energy change due to the MC move is then obtained from conjugate gradient energy minimization carried out with the LAMMPS code [26] using the Fe–C potential. To obey the detailed balance condition, the modified acceptance rule for the MC move from the old (o) to the new (n) state is given by:

$$\text{acc}(o \to n) = \min\left[1, \frac{w(n \to o)}{w(o \to n)} \exp\left(\frac{-E(n) + E(o)}{kT}\right)\right] \tag{2}$$

In Eq. (2), $w(o \to n)$ and $w(n \to o)$ are the probabilities to select the empty site to perform a move from the old state to the new state and vice versa, and $E(n)$ and $E(o)$ are the total energies of the new and old configurations, respectively. As usual, k is the Boltzmann constant and T is the temperature of interest (300 K in this work). As to what concerns structural relaxation, the contribution of the thermal fluctuations of the atomic coordinates is neglected: only the elastic contribution due to carbon insertions is taken into account by means of conjugate gradient optimization. In spite of that, the MC simulations capture the main driving forces for carbon segregation (dislocation-carbon elastic interactions) and local saturation (carbon–carbon chemical interactions). Carbon contents in the 20–500 ppm (0.0005–0.01 wt.%) range are considered. After equilibration, ensemble averages are performed over 10,000 MC steps. When an MC simulation ends, carbon segregation at the screw dislocation is evident, as visually identified in Fig. 1, where the last MC snapshots for $c_0 = 20$, 140 and 500 ppm are shown.

Fig. 2 presents the ensemble-averaged local carbon concentrations near the line defect for some values of c_0. At equilibrium, the carbon atoms in the Cottrell atmosphere are Gaussian-distributed around the dislocation. In the inset of Fig. 2, the linear carbon density along the dislocation core[1] is depicted, indicating that, on average, the core of a screw dislocation is able to absorb up to about 5 carbon atoms per nanometer at 300 K. If the carbon content is low enough ($c_0 \leqslant 50$ ppm), almost all carbon atoms are able to find interstitial positions in the dislocation core. However, as more and more carbon atoms arrive to a volume in the vicinity of the dislocation, carbon–carbon interactions (in general repulsive at short separations, see Refs. [20,22]) play a role as important as carbon-dislocation interactions. This leads to the saturation of that volume, which is not able to accommodate any extra carbon atom. Consequently, the atmosphere starts to spread out, as we observe for $c_0 = 70$ ppm, reaching about 3 nm for $c_0 = 500$ ppm. In the latter, the carbon atoms are distributed in a three-lobed cloud, a feature already reported in three-dimensional atom probe images for a much higher carbon content [27]; Zener ordering is not observed.

Subsequent MD simulations are performed with the LAMMPS code to investigate the effect of segregated carbon on the dislocation mobility, taking the last configurations from MC as models of equilibrated Cottrell atmospheres. In order to make the dislocation glide, shear has to be applied in the direction of the Burgers vector. To this purpose, we follow the procedure used by Domain and Monnet [28]: the iron atoms on one of the free surfaces are displaced with constant velocity in the $(1\,1\,1)$ direction whereas the iron atoms on the opposite free surface are kept frozen in their initial positions. To compute the shear stress σ_{yz} at every MD step, the F_z component of the force acting on the center of mass of the iron atoms on the moving free surface is divided by the total area of the free surface. The simulated physical time is 6 ns (after 1 ns of thermal equilibration), enough to observe the dislocation glide due to the imposed strain rate of $10^7\ \text{s}^{-1}$. Dislocation motion in both the twinning and antitwinning sense was considered.

Fig. 3(a) displays, for each value of c_0, the highest stresses σ_{max}, which are the stresses required to unpin the screw dislocation in the MD simulations. As a general trend, σ_{max} increases with carbon content and, for the same c_0, it is higher when the dislocation glides in the antitwinning sense [29]. However, for very low c_0 – situation in which the dislocation usually has to break free of a single row of carbon atoms in order to glide –, we observe important deviations. This indicates that the force exerted by the carbon atoms arranged on a particular manner in the dislocation core may counterbalance the lattice resistance, thus favouring the glide in the antitwinning sense in some cases. If c_0 is significantly higher, in turn, besides the contribution of the carbon atoms momentarily in the dislocation core, the resulting force also comes from a "tug of

[1] The iron atoms in the core of a screw dislocation are defined by means of the Common Neighbor Analysis criterion.

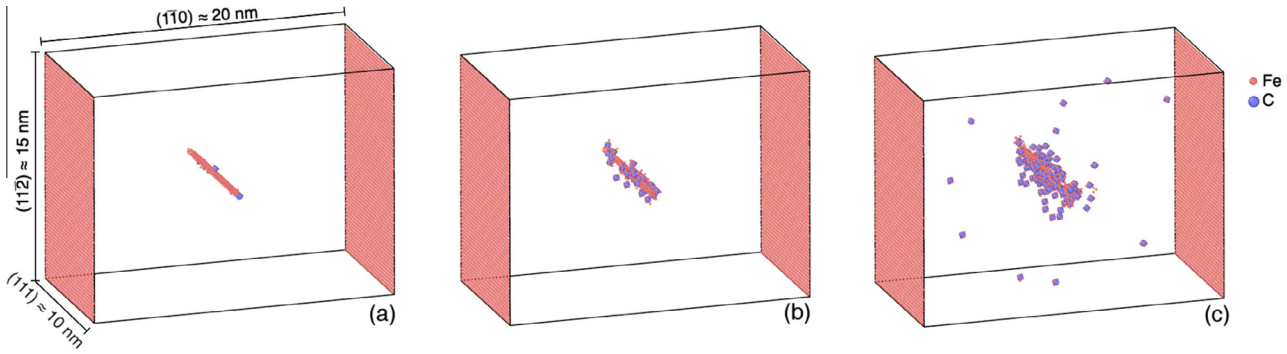

Fig. 1. MC-equilibrated carbon Cottrell atmospheres at $T = 300$ K for the systems with (a) 20, (c) 140 and (b) 500 ppm of carbon. Only non-bcc iron atoms (small red balls) and the carbon atoms (big blue balls) are shown for clarity. (For interpretation of the references to color in this figure legend, the reader is referred to the web version of this article.)

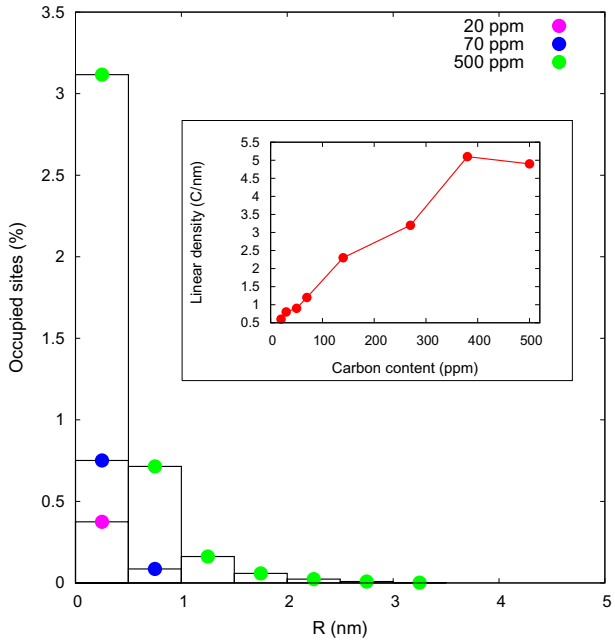

Fig. 2. Ensemble-averaged local carbon concentrations around the screw dislocation. (Inset) Linear density of carbon atoms along the core of the screw dislocation.

war" between the carbon atoms left behind and those still on the dislocation way. At 300 K, the carbon atoms do not have sufficient mobility to follow the line defect. Therefore, as the dislocation moves, the carbon distribution around it becomes skewed and those pulling forces are unbalanced. This behavior differs from that of carbon in solid solution [7], in which only the carbon atoms in the dislocation core effectively anchor the dislocation.

Because of the high strain rate required by MD due to the short physical time that can be simulated, σ_{max} thus obtained is also too high compared with the experimental yield stress [30]. On the other hand, it is worthwhile comparing with MD simulations of carbon in solid solution (the first stage of SSA) to assess how σ_{max} is affected by the atmosphere formation. Fig. 3(b) shows the MD-simulated stress–strain curves corresponding to carbon randomly distributed inside the simulation box and a Cottrell atmosphere, both for $c_0 = 500$ ppm. As the screw dislocation glides through the solid solution, many pinning/unpinning events with the duration of a few picoseconds are present as the dislocation encounters one or more solute atoms on its way, thus resulting in many unpinning stresses. This is in clear contrast with the single pinning/unpinning event of the Cottrell atmosphere system. For

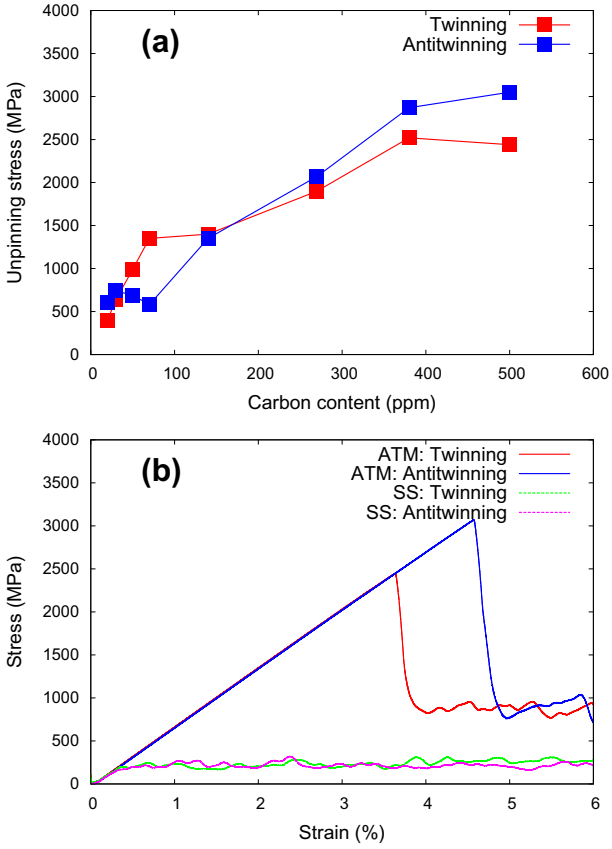

Fig. 3. (a) Stress required to unpin the screw dislocation from the Cottrell atmosphere as a function of carbon content. (b) Stress–strain curves associated with the systems containing 500 ppm of carbon: **ATM** is Cottrell atmosphere; **SS** is solid solution.

$c_0 = 500$ ppm of carbon in solid solution, $\sigma_{max} \approx 270$ MPa, far below σ_{max} of the corresponding Cottrell atmosphere but close to the critical stress in the absence of carbon and the unpinning stress of a single carbon atom (about 200 and 240 MPa, respectively). Therefore a Cottrell atmosphere strongly locks the screw dislocation at its initial rest position. The time it remains immobile also is much longer, in the order of nanoseconds.

The dislocation unpinning from the atmosphere, illustrated in Fig. 4 for $c_0 = 270$ ppm, is a very quick process, not lasting more than a few tens of picoseconds in the MD simulations. When the stress approaches σ_{max}, the kink mechanism comes into play, allowing the dislocation to pass through the carbon cloud up to

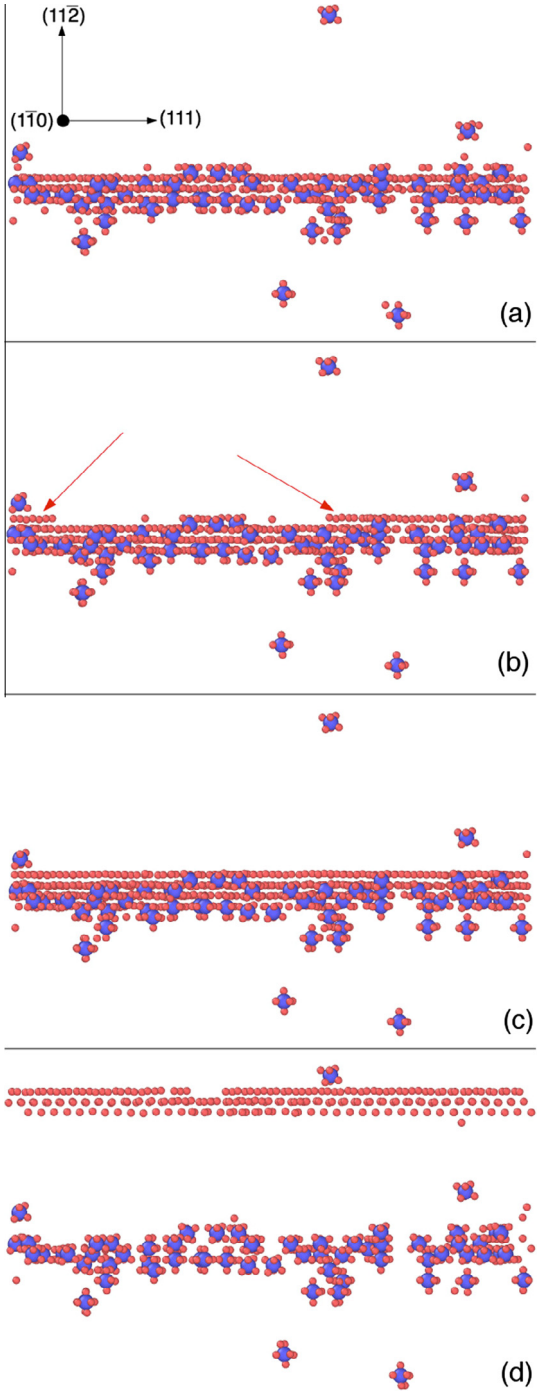

Fig. 4. Dislocation unpinning ($c_0 = 270$ ppm). (a) Immediately before the stress reaches σ_{max}. (b) Dislocation kink (red arrows). (c) The dislocation moves one step from its rest position; σ_{max} is reached. (d) The dislocation is "ejected" from the atmosphere; the stress drops sharply. Only non-bcc iron atoms (small red balls) and the carbon atoms (big blue balls) are shown for clarity. (For interpretation of the references to color in this figure legend, the reader is referred to the web version of this article.)

emerge out of it. Once σ_{max} is reached, the dislocation is suddenly "ejected" from the atmosphere, slowing down after a few picoseconds and then gliding with constant velocity as straining proceeds. In the stress–strain curve, the latter corresponds to the sharp drop in the stress that is characteristic of SSA, in accord with the theory of Cottrell and Bilby.

In conclusion, on-lattice MC revealed strong carbon segregation near a screw dislocation in bcc iron for carbon contents in the 20–500 ppm range. Atomic coordinates corresponding to MC-equilibrated Cottrell atmospheres were used as input coordinates in MD simulations. Particularly for the highest carbon contents of this study, the MD results showed very high unpinning stresses compared to carbon in solid solution. This indicates that, at the end of SSA, screw dislocations end up strongly locked at their rest positions by Cottrell atmospheres, remaining immobile for much longer times and possibly constituting important obstacles to other moving dislocations. In a broad sense, this MC + MD approach can be used to model the role of segregation in a variety of phenomena of interest in materials science (plasticity, grain growth, heat transfer, and so on).

Acknowledgments

R.G.A. Veiga gratefully acknowledges funding by FAPESP "Jovem Pesquisador em Centros Emergentes" Grant 2014/10294-4. This work was carried out within the action CAPES/COFECUB 770/13. The authors would like to acknowledge computing time provided on the Blue Gene/P supercomputer supported by the Research Computing Support Group (Rice University) and Laboratório de Computação Científica Avançada (Universidade de São Paulo).

References

[1] A.H. Cottrell, B.A. Bilby, Proc. Phys. Soc. A (1949) 49–62.
[2] D. Bhattacharya, Metallurgical Perspectives on Advanced Sheet Steels for Automotive Applications, Springer, 2011.
[3] A.K. De, K.D. Blauwe, S. Vandeputte, B.C.D. Cooman, J. Alloys Compd. 310 (2000) 405.
[4] I. Jung, D. Kang, B.C.D. Cooman, Metall. Mater. Trans. A 45 (2014) 1962.
[5] J. Coryell, V. Savic, L. Hector, S. Mishra, SAE Technical Paper (2013) 2013-01-0610.
[6] D. Caillard, J. Bonneville, Scr. Mater. 95 (2015) 15.
[7] H.A. Khater, G. Monnet, D. Terentyev, A. Serra, Int. J. Plast. 62 (2014) 34.
[8] N. Louat, Proc. Phys. Soc. B 69 (1956) 459–467.
[9] A.W. Cochardt, G. Shoek, H. Wiedersich, Acta Metall. 3 (1955) 533–537.
[10] D.M. Barnett, W.C. Oliver, W.D. Nix, Acta Metall. 30 (1982) 673–678.
[11] Y. Hanlumyuang, P.A. Gordon, T. Neeraj, D.C. Chrzan, Acta Mater. 58 (2010) 5481–5490.
[12] R.G.A. Veiga, M. Perez, C.S. Becquart, C. Domain, J. Phys.: Condens. Matter 25 (2) (2013) 025401.
[13] R.G.A. Veiga, M. Perez, C.S. Becquart, E. Clouet, C. Domain, Acta Mater. 59 (2011) 6963.
[14] K. Tapasa, Y.N. Osetsky, D.J. Bacon, Acta Mater. 55 (2007) 93.
[15] E. Clouet, S. Garruchet, H. Nguyen, M. Perez, C.S. Becquart, Acta Mater. 56 (2008) 3450–3460.
[16] E. Clouet, Phys. Rev. B 84 (2011) 224111.
[17] Y.N. Osetsky, D.J. Bacon, Modell. Simul. Mater. Sci. Eng. 11 (2003) 427.
[18] M.S. Daw, M.I. Baskes, Phys. Rev. Lett. 50 (1983) 1285–1288.
[19] G.J. Ackland, M.I. Mendelev, D.J. Srolovitz, S. Han, A.V. Barashev, J. Phys.: Cond. Mat. 16 (2004) S2629.
[20] C.S. Becquart, J.M. Raulot, G. Benecteux, C. Domain, M. Perez, S. Garruchet, H. Nguyen, Comput. Mater. Sci. 40 (2007) 119.
[21] R.G.A. Veiga, C.S. Becquart, M. Perez, Comput. Mater. Sci. 82 (2014) 118–121.
[22] C.W. Sinclair, M. Perez, R.G.A. Veiga, A. Weck, Phys. Rev. B 81 (2010) 224204.
[23] N. Gunkelmann, H. Ledbetter, H.M. Urbassek, Acta Mater. 60 (12) (2012) 4901–4907.
[24] S. Garruchet, M. Perez, Comput. Mater. Sci. 43 (2) (2008) 286–292.
[25] R.G.A. Veiga, M. Perez, C.S. Becquart, C. Domain, S. Garruchet, Phys. Rev. B 82 (2010) 054103.
[26] S.J. Plimpton, J. Comput. Phys. 117 (1995) 1–19.
[27] J. Wilde, A. Cerezo, G.D.W. Smith, Scr. Mater. 43 (2000) 39–48.
[28] C. Domain, G. Monnet, Phys. Rev. Lett. 95 (2005) 215506.
[29] D. Hull, D.J. Bacon, Introduction to Dislocations, fifth ed., Elsevier, 2011.
[30] D.J. Bacon, Y.N. Osetsky, D. Rodney, Dislocations in Solids, Elsevier, 2009 (Ch. 88).